# Adiabatic States of Atomic Hydrogen in Strong Magnetic Fields

Kazuyoshi YAMADA[1,2)]*, Daiji KATO[2,1)]

[1)] *IGSES, Kyushu University, Fukuoka 816-8580, Japan*
[2)] *National Institute for Fusion Science, National Institutes of Natural Sciences, Gifu 509-5292, Japan*

(Received 6 October 2025 / Accepted 20 November 2025)

We calculated adiabatic states of atomic hydrogen in strong magnetic fields treating the radial distance of the spherical coordinates as the adiabatic parameter. The results show a transition from diamagnetic Kepler motion in the inner region to gyromotion along the magnetic field at large distances. At the boundary, avoided crossings of adiabatic potential curves occur along the ridge of the diamagnetic potential, indicating strong local non-adiabatic coupling. These findings clarify the mixed Coulomb-magnetic dynamics of hydrogen and contribute to more accurate modeling of atomic processes in strongly magnetized astrophysical environments.



Keywords: adiabatic basis expansion, strong magnetic field, hydrogen atom

DOI: 10.1585/pfr.21.2401011

## 1. Introduction

Magnetic fields of extraordinary strength, such as those found in neutron-star atmospheres and magnetic white dwarfs, profoundly modify the electronic structure of atoms through Landau quantization and magnetic confinement. Hydrogen, the simplest atom, provides a unique platform for studying these ultra-high-field effects and for interpreting astrophysical spectra [1].

A theoretical framework concerned in the present paper is the *adiabatic basis expansion* method, in which electron motion can be decomposed into fast and slow degrees of freedom. The key idea is to identify one coordinate (the adiabatic parameter) whose variation is relatively slow, and for which the remaining coordinates can be treated as forming an instantaneous eigen-basis, akin to the *Born-Oppenheimer approximation* for molecules. At each fixed value of the adiabatic parameter, the Hamiltonian of the "fast" subsystem is diagonalized, yielding a set of adiabatic eigenfunctions and corresponding potential energy curves that govern the slow motion. High-accuracy implementations of this method have been reported in Refs. [2–5], establishing accurate bound-state energies and photoionization cross sections for hydrogen in strong magnetic fields. The adiabatic basis expansion employing the radial coordinate as an adiabatic parameter has been shown to provide quantitatively reliable results for field strengths up to $B = 10^4 \sim 10^5$ T (typical field strengths of strongly magnetic white dwarfs). On the other hand, no low-field limit is expected with the adiabatic basis expansion method.

However, important challenges remain. First, the hydrogen atom in a magnetic field where both the Coulomb potential and the diamagnetic interaction are important, is a paradigmatic example of *quantum chaos*: classical and quantum analyses reveal the transition from regular to chaotic motion as field strength and excitation energy increase [6, 7]. In such regimes, avoided crossings and strong inter-channel couplings undermine the slow–fast separation assumed in the adiabatic approach, leading to possible inaccuracies and convergence problems. Zhao *et al.* themselves pointed out cross-method discrepancies in this parameter range [5].

These theoretical uncertainties directly affect the modeling of *hydrogen absorption features observed in strongly magnetized stars*. Detailed atmosphere models and X-ray/optical observations of isolated neutron stars (*e.g.*, Ref. [8]) and magnetic white dwarfs (*e.g.*, Ref. [9]) rely critically on accurate bound-free and bound-bound opacities of hydrogen in fields up to $10^9$ T. Discrepancies in theoretical level energies or transition strengths translate into uncertainties in inferred surface temperatures, magnetic field strengths, and compositions of these stars.

In the present study, we focus specifically on the *adiabatic eigenfunctions* that constitute the core of the adiabatic basis expansion. In the following sections, we introduce the adiabatic basis expansion method in spherical coordinates and present a numerical scheme to solve the adiabatic eigenvalue equations accurately. The results of the present calculations are then shown for an intermediate field strength of 470 T where the adiabatic basis expansion method is expected to be the most accurate. The physical and topological properties of

*Corresponding author's e-mail: yamada.kazuyoshi.499@s.kyushu-u.ac.jp
This article is based on the presentation at the Joint Conference of the 22nd International Conference on Atomic Processes in Plasmas (APiP 2025) and 1st NIFS Conference on Atomic and Molecular Processes in Plasmas.
The presentation was selected as APiP2025 Best Student Poster.

these adiabatic states as a function of an adiabatic parameter will be discussed.

Throughout this paper, atomic units (a.u.) are adopted, i.e., $\hbar = m_e = e = 1$, unless otherwise noted.

## 2. Theoretical Method

Firstly, we derive the Schrödinger equation for a *spinless* electron moving in the attractive Coulomb field of a proton and a uniform magnetic field with spherical coordinates,

$$x = r\sin\theta\cos\phi,\ \ y = r\sin\theta\sin\phi,\ \ z = r\cos\theta$$
$$r = \sqrt{x^2 + y^2 + z^2} \quad . \tag{1}$$

Electron wave functions in the sperical coordinates are written in the following form, assuming the magnetic field along $z$,

$$\Psi(r,\theta,\phi) = r^{-1}\psi(r,\theta)\,e^{im\phi}, \tag{2}$$

where $m$ is the magnetic quantum number. The two-dimensional Schrödinger equation for $\psi(r,\theta)$ reads,

$$\left[-\frac{1}{2}\left(\frac{\partial^2}{\partial r^2} - \frac{\hat{l}^2}{r^2}\right) + V(r,\theta) - E\right]\psi(r,\theta) = 0, \tag{3}$$

where $\hat{l}^2$ is the squared angular momentum operator, and the interaction potential $V(r,\theta)$ is expressed as

$$V(r,\theta) = -\frac{1}{r} + \frac{m}{2}\gamma + \frac{1}{8}\gamma^2(r\sin\theta)^2, \tag{4}$$

where $\gamma = B_z/B_0$, ($B_0 \approx 2.35 \times 10^5$ T). Figure 1 shows the interaction potential for $B_z$ = 470 T ($\gamma \approx 0.002$). Near the origin, the Coulomb potential of the nucleus dominates and exhibits spherical symmetry, whereas at a large distance, the diamagnetic interaction potential becomes dominant and exhibits cylindrical symmetry. An accurate numerical method, which can be used for both bound and continuum states, is sought for non-integrable systems exhibiting such mixed symmetries.

Ignoring radial kinetic energy, we define the adiabatic equation for angular motion of the electron at a fixed $r$,

$$\left[\frac{\hat{l}^2}{2r^2} + V(r,\theta)\right]\varphi_\mu(\theta;r) = U_\mu(r)\,\varphi_\mu(\theta;r), \tag{5}$$

where $\varphi_\mu$ and $U_\mu$ are adiabatic channel functions and adiabatic potential energies as a function of $r$, respectively. The solutions of non-separable two-dimensinal Schrödinger equation (Eq. (3)) are expanded with the adiabatic channel functions at each $r$ (adiabatic basis expansion),

$$\psi(r,\theta) = \sum_\mu F_\mu(r)\,\varphi_\mu(\theta;r)\,. \tag{6}$$

In the present work, the adiabatic equation (Eq. (5)) is solved by *Rayleigh-Ritz variational principle* with the spherical harmonics $Y_{lm}$,

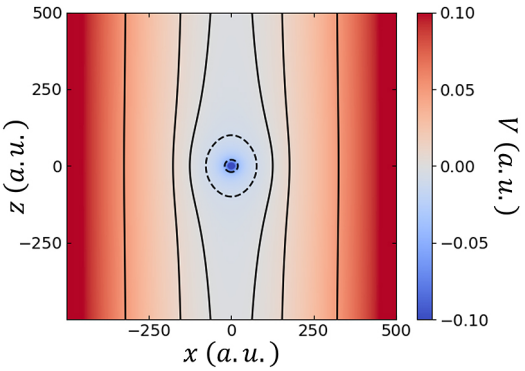


Fig. 1. Contour map of interaction potential energies on the $x$–$z$ plane for $B_z$ = 470 T ($\gamma \approx 0.002$).

$$\varphi_\mu(\theta;r)\,e^{im\phi} = \sum_l c_l(r)\,Y_{lm}(\theta,\phi), \tag{7}$$

where $l \geq 0$ is the azimuthal quantum number. The channel function of nonzero $|m|$ represents the polar amplitude of a vortex electron with a *topological charge* equal to $m$.

The expansion coefficients $\mathbf{c} = \{c_l\}$ and the adiabatic potential energies are obtained as solutions of the eigenvalue problem,

$$\mathbf{Ac} = U_\mu\mathbf{c}, \tag{8}$$

where the matrix elements of $\mathbf{A}$ are

$$A_{l'l} = \left[\frac{l(l+1)}{2r^2} - \frac{1}{r} + \frac{m\gamma}{2} + \frac{\gamma^2 r^2}{12}\right]\delta_{l'l} - (-1)^{-m}\frac{\gamma^2 r^2}{12}\sqrt{(2l'+1)(2l+1)}\times \cdot \begin{pmatrix} l' & 2 & l \\ 0 & 0 & 0 \end{pmatrix}\begin{pmatrix} l' & 2 & l \\ -m & 0 & m \end{pmatrix} \tag{9}$$

Wigner's $3j$ symbols in the RHS of Eq. (9) equal to zero unless $l' + l \geq 2$ and $|l' - l| \leq 2$, and $l' + l$ are even integers. Therefore, even and odd $l$ elements of $\mathbf{A}$ are decoupled; the spatial inversion symmetry is conserved (Parity conservation).

## 3. Results and Discussion

First, we checked the convergence of the adiabatic potential energies for $B_z$ = 470 T with respect to the number of spherical harmonics, $n_b$, in the adiabatic channel functions. The convergence was evaluated at large $r$ where a greater number of spherical harmonics are required to obtain converged results. Figure 2 indicates that each of the 16 lowest adiabatic potential energies calculated at $r$ = 500 is converged for $n_b \geq 100$. All subsequent results in the present work are, therefore, obtained using $n_b$ = 150. In Fig. 3, the lowest 16 adiabatic potential energy curves are plotted as a function of $r$. Near the origin, the adiabatic potential energy curve can be approximated by the centrifugal potential, and at large distances, it converges to the Landau levels with the constant interval of $\gamma$ [10]. Note that Landau levels with even and odd

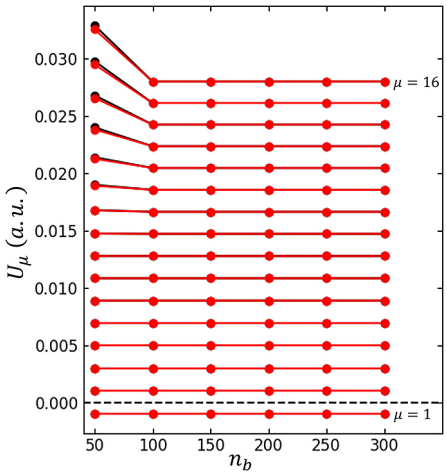


Fig. 2. Adiabatic potential energy $U_\mu$ ($\mu$ = 1–16, $m$ = 0) at $r$ = 500 with respect to number of basis function $n_b$. Black: even parity, and red: odd parity.

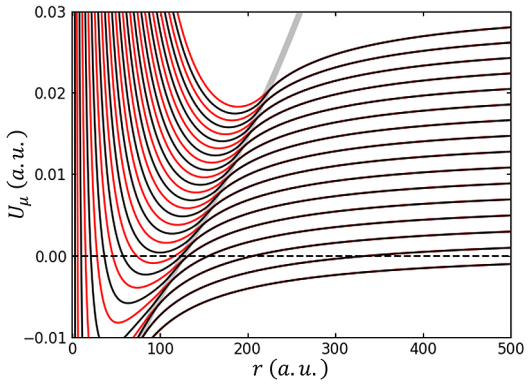


Fig. 3. Adiabatic potential energy $U_\mu$ ($\mu$ = 1–16, $m$ = 0) and avoided-crossing sequence. Black: even parity, and red: odd parity.

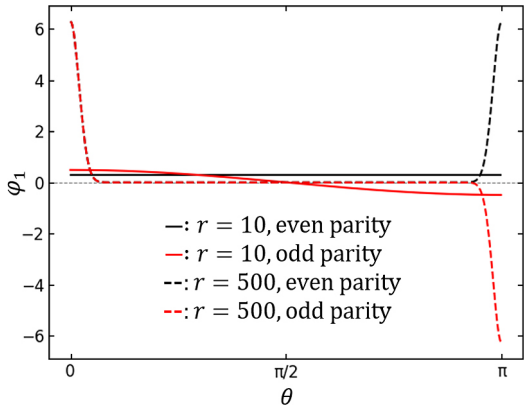


Fig. 4. The lowest adiabatic channel function $\varphi_1$ ($m$ = 0). Black: even parity, and red: odd parity. Solid curves show amplitudes at $r$ = 10, and dashed curves at $r$ = 500.

parity are degenerate.

The behavior of the channel function amplitude can also be approximated by spherical harmonics at small $r$, but at large distances it tends to localize near $\theta$ = 0, π (near the $z$-axis) due to the strong diamagnetic interaction, as illustrated in Fig. 4. The channel functions with no node or an even number of nodes are symmetric about $\theta$ = π/2 (even parity), whereas those with an odd number of nodes are antisymmetric (odd parity). The number of nodes in each channel function is conserved independently of $r$.

Figure 5 shows squared amplitudes of the lowest channel functions of even parity for $|m|$ = 0, 10, 20 plotted on spheres. For nonzero magnetic quantum numbers ($|m| \neq 0$), there is a phase singularity on the $z$-axis where the channel function has no amplitude. Around this point, the phase varies continuously and typically winds by an integer multiple of 2π, i.e., $e^{im\phi}$. The integer winding number $m$ defines the topological charge of the singularity. At the small $r$, the squared amplitude represents a polar distribution of the stretched state ($|m| = l$), and at the large distance, it represents that of the Landau state.

Change in the amplitudes of the channel functions reflect a transformation in the dynamics that governs the adiabatic state. Specifically, in the region where $r$ is small, it exhibits the diamagnetic Kepler motion of the electron in the Coulomb field (central force) of the nucleus, while at large distances it shows gyromotion along the magnetic field. The adiabatic potential energy curve connects each adiabatic state with the same number of nodes in these two regimes, akin to the interatomic potential energy curve in the Born-Oppenheimer approximation for molecules. However, a sharp boundary between the two regimes is observed in the adiabatic potential energy curves (indicated by the gray curve in Fig. 3). Avoided-crossings of adjacent potential curves distribute as if tracing this boundary where *non-adiabatic* couplings of channels with the same parity and the magnetic quantum number $m$ occurs locally.

We investigated the mechanism behind the locally distributed avoided-crossing sequence. As can be seen from Eq. (4), at a fixed $r$, the diamagnetic potential reaches its maximum (*potential ridge*) on the plane perpendicular to the magnetic field at $z$ = 0 ($\theta$ = π/2). We heuristically express an effective potential energy of an electron on the potential ridge as the sum of the centrifugal potential for the stretched state near the origin and the interaction potential,

$$U_{ridge} = \frac{l(l+1)}{2r^2} + V(r, \theta = \pi/2). \quad (10)$$

In Fig. 6, the ridge potential curves for $l$ = 0, 10, 20 subtracted by the paramagnetic term: $U_{ridge} - m\gamma/2$, are plotted along with the corresponding adiabatic potential energy curves. As can be seen in the figure, the ridge potential curve accurately traced the avoided crossings of each $|m| = l$. This result indicates that the non-adiabatic coupling is occurring locally along the potential ridge. Note that the effective potential on the $z$ = 0 plane is also known to give the correct interval of the *quasi-Landau resonances* observed in photoabsorption spectra of Rydberg atoms [11] which is 1.5 times larger than that of the Landau levels at $E$ = 0, i.e., 1.5$\gamma$ (*e.g.*, Ref. [12]).

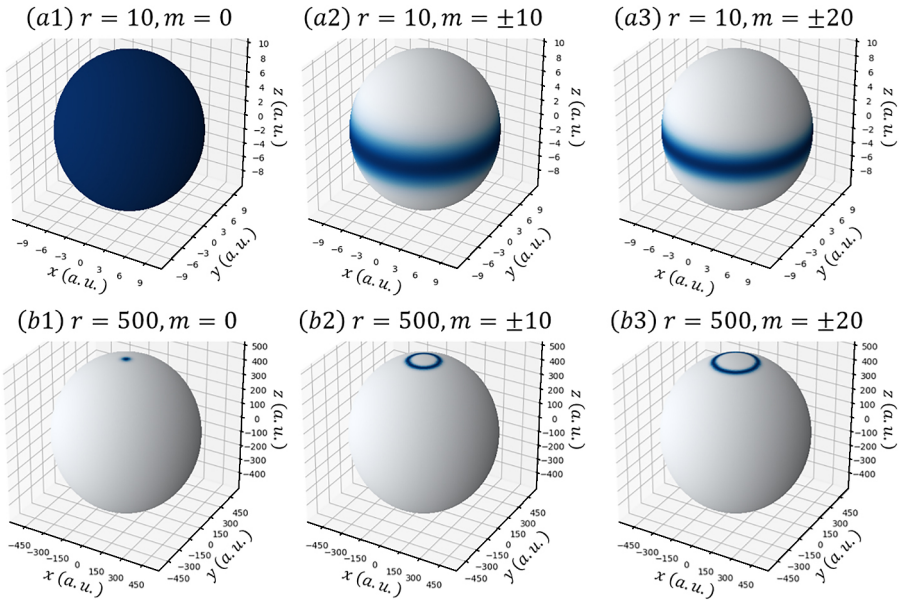


Fig. 5. Spherical color map for the squared amplitudes of the lowest adiabatic channel functions $\varphi_1^2$ of even parity at $r$ = 10 and 500, for $|m|$ = 0 ($a1$, $b1$), 10 ($a2$, $b2$), and 20 ($a3$, $b3$). The color scale is normalized for each panel.

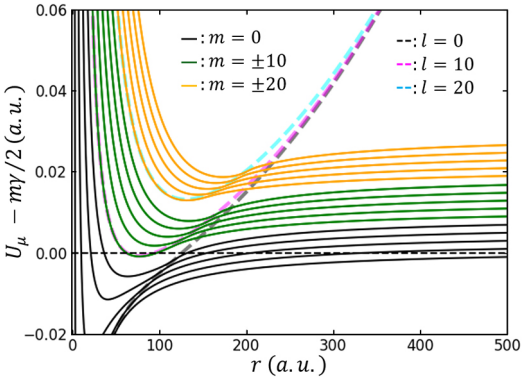


Fig. 6. The lowest 5 adiabatic potential energy curves subtracted by the paramagnetic term: $U_\mu - m\gamma/2$, for $|m|$ = 0, 10, 20. Dashed lines are the ridge potential (Eq. (10)) for $l$ = 0, 10, 20 subtracted by the paramagnetic term.

## 4. Conclusion

We studied the properties of adiabatic states for atomic hydrogen in a strong magnetic field. The adiabatic channel functions and potential energies were numerically obtained treating the radial distance of the spherical coordinates as the adiabatic parameter. It was shown that the channel functions and potential energies represent both the diamagnetic Kepler motion of the bound electron in the inner region and the gyromotion along the magnetic field at large distances. This study has revealed that the transition between the two motions occurs via avoided-crossings of the adiabatic potential curves formed along the ridge of the diamagnetic interaction potential, where non-adiabatic coupling of the channels is important. These findings have important implications for the development of accurate numerical methods for photoionization and radiative recombination, where both the diamagnetic Kepler motion and gyromotion interplay.

This work is supported by the NIFS collaboration program (NIFS25KSPQ004). KY is grateful for financial supports by the JST SPRING (Grant Number JPMJSP2136) and the Kuma Science Engineering and Culture Promotional Foundation.

[1] H. Ruder *et al.*, *Atoms in Strong Magnetic Fields: Quantum Mechanical Treatment and Applications in Astrophysics and Quantum Chaos* (Springer, 1994).
[2] S. Watanabe and H. Komine, Phys. Rev. Lett. **67**, 3227 (1991).
[3] M. Mota-Furtado and P.F. O'Mahony, Phys. Rev. A **76**, 053405 (2007).
[4] O. Chuluunbaatar *et al.*, J. Phys. A: Math. Theor. **40**, 11485 (2007).
[5] L.B. Zhao *et al.*, Phys. Rev. A **103**, 022807 (2021).
[6] D. Delande and J.C. Gay, Phys. Rev. Lett. **57**, 2006 (1986).
[7] H. Friedrich and D. Wintgen, Phys. Rep. **183**, 37 (1989).
[8] W.C.G. Ho and D. Lai, Mon. Not. R. Astron. Soc. **327**, 1081 (2001).
[9] A.Y. Potekhin *et al.*, Astrophys. J. **612**, 1034 (2004).
[10] L.D. Landau and E.M. Lifshitz, *Quantum Mechanics: Nonrelativistic Theory* (Elsevier, Amsterdam, 1981).
[11] W.R. Garton and F.S. Tomkins, Astrophys. J. **158**, 839 (1969).
[12] J.A.C. Gallas and R.F. O'Connell, J. Phys. B: At. Mol. Phys. **15**, L75 (1982).